AGU PUBLICATIONS

Geophysical Research Letters

RESEARCH LETTER
10.1002/2014GL060183

Key Points:
- Lake level reconstructions show coherent multicentury hydrologic variation
- Four multicentury droughts in the northeast U.S. after ~5.6 ka
- Variability with pan-Atlantic climate changes preceded high water levels today

Supporting Information:
- Readme
- Table S1
- Text S1

Correspondence to:
P. E. Newby,
Paige_Newby@brown.edu

Citation:
Newby, P. E., B. N. Shuman, J. P. Donnelly, K. B. Karnauskas, and J. Marsicek (2014), Centennial-to-millennial hydrologic trends and variability along the North Atlantic Coast, USA, during the Holocene, *Geophys. Res. Lett.*, *41*, 4300–4307, doi:10.1002/2014GL060183.

Received 21 APR 2014
Accepted 4 JUN 2014
Accepted article online 9 JUN 2014
Published online 25 JUN 2014

Centennial-to-millennial hydrologic trends and variability along the North Atlantic Coast, USA, during the Holocene

Paige E. Newby[1], Bryan N. Shuman[2], Jeffrey P. Donnelly[3], Kristopher B. Karnauskas[3], and Jeremiah Marsicek[2]

[1]Department of Geological Sciences, Brown University, Providence, Rhode Island, USA, [2]Department of Geology and Geophysics, University of Wyoming, Laramie, Wyoming, USA, [3]Department of Geology and Geophysics, Woods Hole Oceanographic Institution, Woods Hole, Massachusetts, USA

Abstract Geophysical and sedimentary records from five lakes in Massachusetts reveal regionally coherent hydrologic variability during the Holocene. All of the lakes have risen since ~9.0 ka, but multicentury droughts after 5.6 ka repeatedly lowered their water levels. Quantified water level histories from the three best-studied lakes share >70% of their reconstructed variance. Four prominent low-water phases at 4.9–4.6, 4.2–3.9, 2.9–2.1, and 1.3–1.2 ka were synchronous across coastal lakes, even after accounting for age uncertainties. The droughts also affected sites up to ~200 km inland, but water level changes at 5.6–4.9 ka appear out of phase between inland and coastal lakes. During the enhanced multicentury variability after ~5.6 ka, droughts coincided with cooling in Greenland and may indicate circulation changes across the North Atlantic region. Overall, the records demonstrate that current water levels are exceptionally high and confirm the sensitivity of water resources in the northeast U.S. to climate change.

1. Introduction

Multicentury hydroclimate variability is an important, but poorly constrained, feature of the warm climates of the Holocene and other interglacials [*Fawcett et al.*, 2011]. Understanding the timing, spatial patterning, magnitude, and causal mechanisms of such variability will help to clarify the spectrum climate change [*Wanner et al.*, 2011; *Shuman*, 2012] and the potential for persistent changes in societally significant water resources [*Milly et al.*, 2008]. Lake level reconstructions can address these needs because they directly record past changes in the balance of precipitation and evaporation (referred to here as effective moisture) [*Harrison and Digerfeldt*, 1993] and extend knowledge of hydroclimatic change to timescales and frequencies well beyond the reach of instrumental, dendroclimatic, and other archives [*Cook et al.*, 2007].

The coherence of lake level reconstructions with each other and with other paleoclimate records has been difficult to assess on multicentennial scales, however, because of (i) limited temporal resolution and age control, (ii) a lack of replication required to differentiate regional climatic signals from internal variation at core-to-watershed scales, and (iii) a wide range of reconstruction approaches, validation, and uncertainty [*Fritz et al.*, 2000a, 2000b; *Shuman and Finney*, 2006]. We, therefore, apply systematic event-synchrony and paleohydrologic analyses [*Parnell et al.*, 2008; *Pribyl and Shuman*, 2014] to multiple lakes in the northeast U.S. to test the assumption that detailed and well-dated lake sediment stratigraphies capture a coherent signal of centennial-to-millennial hydrologic change. The analyses depend upon the observation that nearshore (littoral) sands extend outward from a lake's shore during periods of low water and that deepwater muds expand shoreward during periods of high water [*Digerfeldt*, 1986; *Newby et al.*, 2009, 2011; *Marsicek et al.*, 2013; *Pribyl and Shuman*, 2014]. We evaluate whether the timing of such changes are regionally coherent and whether they coincide with climate variability in the North Atlantic region, such as observed on decadal timescales [*Bradbury et al.*, 2002; *Seager et al.*, 2012].

Existing lake and pollen data indicate that recent moist conditions followed a long-term rise in effective moisture throughout the Holocene, which resulted from multimillennial changes in seasonal insolation and the Laurentide Ice Sheet [*Webb et al.*, 1993; *Shuman and Plank*, 2011; *Marsicek et al.*, 2013]. Less is known about variability superimposed upon the orbital-scale trend, but North Atlantic variability has been implicated as a driver of regional droughts at annual to decadal scales [*Namias*, 1966; *Enfield et al.*, 2001; *Feng et al.*, 2010;

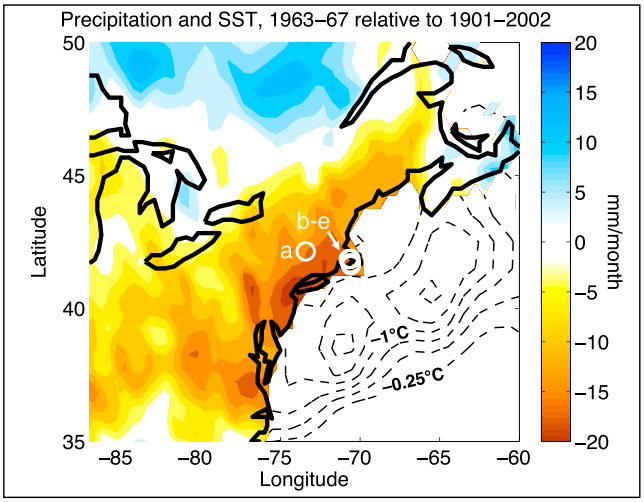

Figure 1. Map shows locations of study sites (a = Davis, b = New Long, c = Round, d = Flax, and e = Deep Ponds) along with the mean observed sea surface temperature (SST) and precipitation anomalies of the A.D. 1963–1967 drought (relative to a base period of 1901–2002). SST anomalies (black contours) are contoured every 0.25°C, and precipitation values correspond to the color bar based on the HadISST1 [*Rayner et al.*, 2003] and University of East Anglia Climate Research Unit TS2.1 [*Mitchell and Jones*, 2005] data sets.

Seager et al., 2012]. For example, the severe A.D. 1960s drought coincided with a persistently negative phase of the North Atlantic Oscillation (NAO) and anomalously low sea surface temperatures (SST) off the eastern Atlantic seaboard (Figure 1) [*Namias*, 1966; *Seager et al.*, 2012]. Past droughts could have persisted for decades to centuries [*Li et al.*, 2007; *Newby et al.*, 2009, 2011; *Pederson et al.*, 2013] because North Atlantic atmospheric and ocean circulation probably also shifted in similar ways on decadal-to-multicentennial timescales during the Holocene [*O'Brien et al.*, 1995; *Thornalley et al.*, 2009; *Martin-Puertas et al.*, 2012].

Here we synthesize the evidence of paleohydrologic changes at coastal and inland sites in the northeast U.S. We consider evidence from ground-penetrating radar (GPR) data and sediment cores, reconstruct and compare lake level changes, and analyze the uncertainty associated with the timing of low-water episodes. We then discuss how the patterns of hydrologic change compare with climate variability in the North Atlantic region [e.g., *Alley*, 2000].

2. Approach

2.1. Geophysical and Sedimentary Data

We collected GPR data from small kettle lakes across Massachusetts (Figure 1) to detect stratigraphic changes consistent with lake level change. GPR profiles show stratigraphic boundaries (radar reflectors) associated with changes in sediment dielectric properties and illustrate the geometries of the stratigraphic units within each lake basin. Strong reflections and the truncation of units nearshore can indicate sand layers and unconformities formed during water level fluctuations.

We show representative GPR profiles (Figure 2) from New Long and Davis Ponds from eastern and western Massachusetts, respectively, [*Newby et al.*, 2009, 2011] and compare them with representative examples of unpublished profiles from other sites, such as Round and Flax Ponds. None of the lakes have surface stream inputs or outflow. Each represents a surface expression of the local groundwater, which ensures that the stratigraphic changes are linked to climatically influenced groundwater fluctuations rather than changes in sediment delivery [*Pribyl and Shuman*, 2014]. The profiles were collected using a Geophysical Survey System, Inc. Subsurface Interface Radar-2000 GPR with 200 and 400 MHz antennas floated on the surface of the ponds.

X-radiography of cores from New Long (NLP), Davis, and Round Ponds are used to confirm that prominent reflectors in the GPR profiles represent basinward expansion of sandy facies (Figure 2). X-radiographs and elemental data were obtained using an ITRAX X-ray fluorescence (XRF) core scanner at Woods Hole Oceanographic Institution. We review representative core data (Figure 3) to describe the stratigraphic changes at NLP and a fourth eastern lake, Deep Pond [*Newby et al.*, 2009; *Marsicek et al.*, 2013]. The timing of the stratigraphic changes is based on 52 calibrated accelerator mass spectrometry radiocarbon dates from NLP [*Newby et al.*, 2009], 53 dates from Deep Pond [*Marsicek et al.*, 2013], 31 dates from Davis Pond [*Newby et al.*, 2011], and 9 dates from Round Pond (Table S1).

2.2. Lake Level Reconstruction

The water level histories of NLP (in the coastal Plymouth-Carver aquifer), Deep Pond (in the coastal Cape Cod aquifer), and Davis Pond (in the inland Berkshire Hills) have been approximated previously [*Newby et al.*, 2009, 2011;

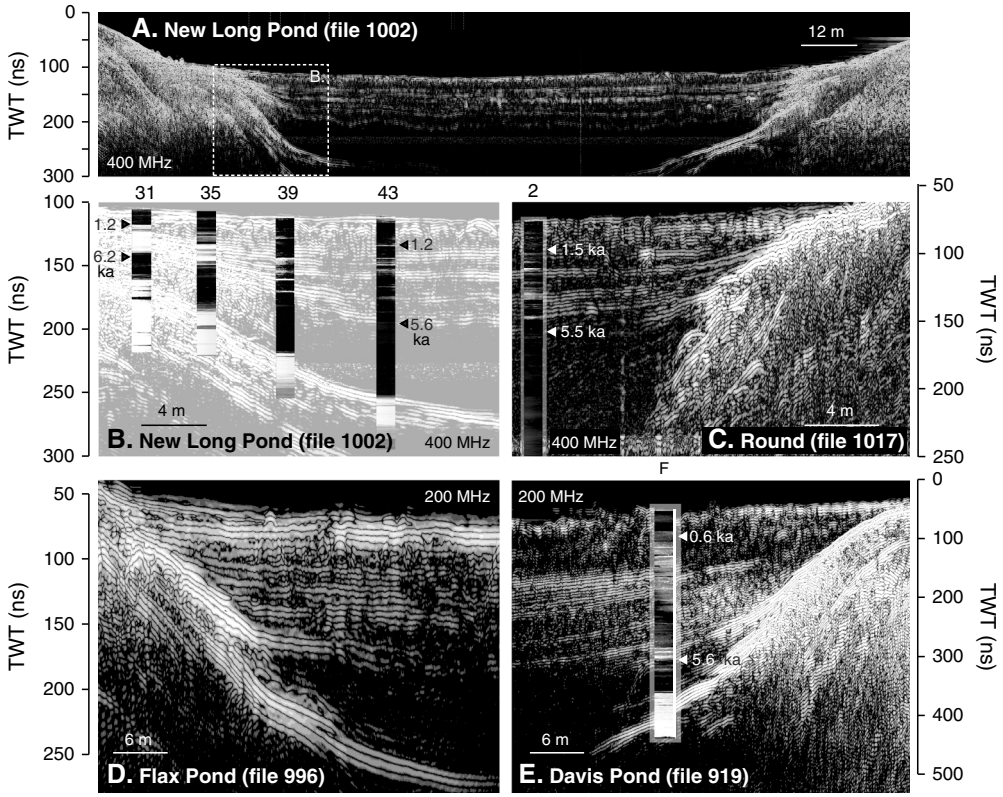

Figure 2. (a) GPR profile across New Long Pond (NLP), Massachusetts, shows the subaqueous sediment stratigraphy including multiple bright reflectors, which correspond to sand layers (paleoshorelines) that extend out from shore. (b) The stippled white square in Figure 2a is enlarged and compared with X-radiographs from four cores, which contain sand layers (indicated by white intervals). Cores are labeled by their distance in meters from shore. Triangles denote the position of representative calibrated radiocarbon ages, which bracket the interval of greatest stratigraphic variability. Three additional GPR profiles and X-radiographs of cores from (c) Round, (d) Flax, and (e) Davis Ponds show the most shoreward portion of each basin and contain stratigraphies similar to NLP.

Marsicek et al., 2013], but here we quantify and statistically compare the reconstructions. To do so, we use a decision-tree approach to iteratively interpret data from multiple radiocarbon-dated sediment cores at each lake, identify littoral facies in the cores, and constrain the past elevations of the littoral zone and, thus, the water levels [*Marsicek et al*., 2013; *Pribyl and Shuman*, 2014]. Incorporating the elevations of the cores through time accounts for the increasing sensitivity of individual cores to water level changes (i.e., a bias toward accumulating sands) as sediments accumulate and core locations shallow. Water depth indicated by facies type depends upon both climate and sediment infilling, but water surface elevation, indicated by the minimum elevation of littoral facies in multiple cores, depends only upon climate [*Winter*, 1999; *Pribyl and Shuman*, 2014]. We use cross-site linear regression and correlation analyses focused on the mean lake level reconstructions but also show the 1 sigma uncertainty ranges of the reconstructions.

Our reconstructions depend upon data from two cores at NLP [*Newby et al*., 2009], four at Deep Pond [*Marsicek et al*., 2013], and six at Davis Pond [*Newby et al*., 2011]. At Davis and Deep Ponds, we rely on loss on ignition (LOI) from the sediment at 550°C because LOI is reduced in nearshore cores from >50% to <25% at the onset of the low-water events when sand extended outward from shore [*Newby et al*., 2011; *Marsicek et al*., 2013]. At NLP, XRF counts of titanium (Ti) provide more detail than the correlated LOI and sand content data [*Newby et al*., 2009]. Ti counts >50 exceed mean background levels in deepwater silts at NLP by >1 standard deviation and are used to define the timing of low water.

2.3. Age Uncertainties

We compare age uncertainty distributions associated with multicentury water level variability based on major lithostratigraphic changes within (i) individual cores at NLP and Davis Pond (43 and 100 m from shore, respectively)

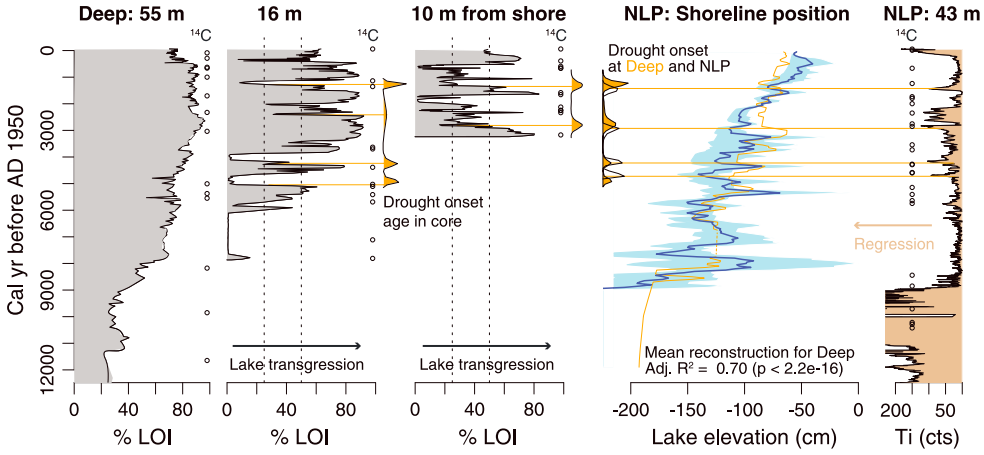

Figure 3. Representative sediment core stratigraphies from Deep Pond and New Long Pond (NLP) indicate periods of lake transgression and regression. Low loss on ignition (LOI) data from Deep Pond cores 55, 16, and 10 [*Marsicek et al.*, 2013] and high titanium (Ti) counts from NLP core 43 [*Newby et al.*, 2009] indicate shallow water sands. The systematic water level reconstruction with uncertainty is shown in blue for NLP; the mean reconstruction for Deep Pond is plotted (in orange) based on a linear regression onto the mean NLP curve. Filled orange age distributions show the timing of the onset of shallow water in cores 16 and 10 at Deep Pond; horizontal orange lines denote the midpoint of the associated decreases in LOI from >50% to <25%. For comparison, the summed age distributions from both Deep Pond cores are plotted with the age distributions (black, unfilled curve) of the equivalent sedimentary transitions in NLP core 43 (increases in Ti counts to >50). Circles denote the position of calibrated radiocarbon ages from each core.

and (ii) two cores at Deep Pond (16 and 10 m from shore). The comparisons show whether climatic rather than site-specific factors caused the hydrologic and stratigraphic changes across cores, different watersheds, and aquifers. Specifically, we test for asynchrony by generating 10,000 possible ages for each stratigraphic change using a Bayesian approach to resample from and random walk between the calibrated radiocarbon ages in each core [*Parnell et al.*, 2008]. By comparing the distributions of possible ages, we assessed whether asynchrony in the onset and termination of periods of low water could be ruled out with >95% confidence [*Parnell et al.*, 2008]. Modal sample ages are presented here to represent the beginning and end of drought periods and are rounded to 5 year intervals.

3. Results

3.1. Regional Similarities in GPR Stratigraphies

GPR profiles from kettle lakes and other groundwater-fed ponds throughout the northeast U.S. reveal subsurface stratigraphies with multiple, closely spaced radar reflectors extending laterally out from shore (Figure 2). The features meet the expectations for evidence of water level changes [*Pribyl and Shuman*, 2014] because they extend from multiple sides of each lake and include reflectors truncated by expansion of the nearshore erosive zone during low water.

At NLP, like multiple other sites, an upper unit of closely spaced, horizontal reflectors overlies a radar-transparent interval with few reflectors (Figure 2a). An enlargement of the western nearshore section from this profile (Figure 2b) highlights the correspondence of the upper, closely spaced reflectors to sand layers deposited from ~5.6–1.2 ka, which appear as bright layers in the X-radiographs of the NLP cores. The layers coalesce nearshore, and few are apparent below the 5.6 ka horizon (Figure 2b).

GPR profiles and core X-radiographs from Round Pond, located in the same glacial-outwash aquifer as NLP (Figure 1), contain a similar sequence of multiple reflectors and sand layers from 5.5 to 1.5 ka above a radar-transparent sequence of fine silts (Figure 2c). Flax Pond, located in a different aquifer within a moraine (rather than outwash sands) in southeastern Massachusetts, also shows a consistent sequence of closely spaced reflectors above a uniform, radar-transparent interval (Figure 2d). Other lakes in the region, such as Crooked, Rocky, and Deep Ponds, also show similar GPR stratigraphies [*Shuman and Donnelly*, 2006; *Newby et al.*, 2009; *Marsicek et al.*, 2013], as do GPR profiles from lakes in western Massachusetts and Connecticut, such as Davis Pond (Figure 2e). Davis Pond is located on glaciolacustrine deposits and also contains multiple thin reflectors above a radar-transparent interval deposited before 5.6 ka.

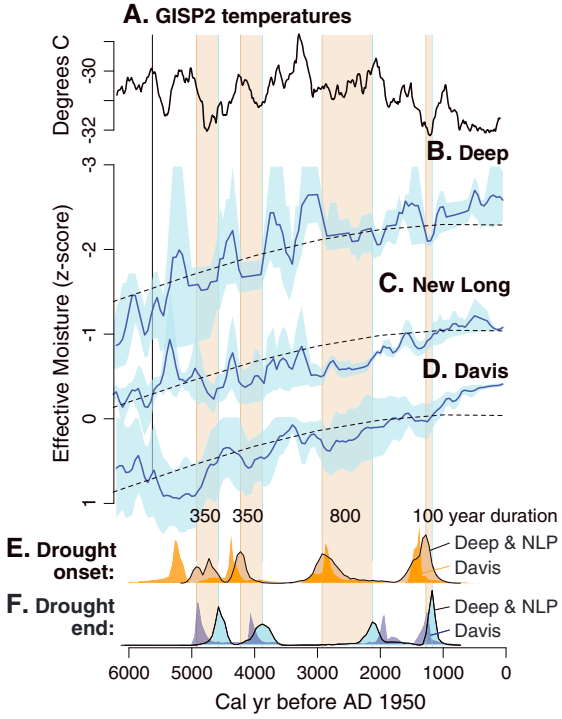

Figure 4. (a) Greenland temperatures since 6.0 ka [*Alley*, 2000] are compared with the reconstructed water level histories (plotted as *z* scores) from (b) Deep (offset by +1 standard deviation unit), (c) New Long, and (d) Davis Ponds (offset by −1 standard deviation unit). Shaded vertical bars indicate periods of centennial-to-millennial drought defined by the modal ages of the (e) onset (tan histograms) and (f) termination (light blue histograms) of nearshore sand layers at Deep and New Long Ponds. For comparison, age distributions of the onset shown in Figure 4e (dark orange) and termination shown in Figure 4f (dark blue) of sand accumulation in the central core (A100) from Davis Pond are also shown. Dash lines show insolation trends (inverted) regressed onto the lake level reconstructions (adjusted R^2 values range from 0.60 to 0.76).

3.2. Consistent Water Level Changes in Eastern Massachusetts

The radiocarbon ages from multiple cores collected along the GPR transects provide chronologic constraints on the features in the radar stratigraphies. At NLP (Figure 2b), repeated middle to late Holocene low-lake stands generated layers of sandy, littoral sediments that extended outward into the lake and truncated underlying organic-rich mud [*Newby et al.*, 2009]. Both X-radiography (Figure 2b) and Ti count data (Figure 3) from NLP indicate at least four centennial-to-millennial periods since 5.0 ka when sands were deposited as far as core 43.

Ti counts increased to >50 from background levels beginning at 4.725, 4.175, 2.925, and 1.475 ka. Based on the radiocarbon-dated changes in NLP cores 43 and 31, our decision-tree approach estimates that the Ti peaks in NLP core 43 represent 25–50 cm declines in the lake's elevation amid a >200 cm increase since 9.0 ka (Figure 3). The uppermost Ti peak (>200 counts) extends above a high historic background Ti level related to local land use and has a median age of −0.013 ka consistent with the A.D. 1960s drought (Figures 3 and 1) [*Newby et al.*, 2009].

LOI data from Deep Pond [*Marsicek et al.*, 2013] represent a similar sequence of lake level changes on Cape Cod, Massachusetts (Figure 3). Transgressions of the lake initiated high-LOI silt accumulation between four prominent low-LOI sand layers deposited during regressions after 4.925, 4.250, 2.800, and 1.275 ka in cores 16 and 10 m from shore. The upper sand layer illustrates the internal consistency of the ages of the major facies changes and began to accumulate at 1.275 (1.375–1.225) and 1.350 (1.590–0.930) ka in cores 16 and 10, respectively (Figure 3). These changes in facies are not recorded in a core collected at the center of the pond (55 m from the shore), indicating continuous accumulation in deep water even during times when water levels were low (Figure 3).

The quantified lake level reconstructions from NLP and Deep Pond are well correlated ($r = 0.91 \pm 0.07$) (Figure 3). Both capture similar long-term water level increases since >9.0 ka and four multicentury low-water episodes since 5.0 ka (Figures 3 and 4).

3.3. Water Level Changes in Western Massachusetts

Nearshore cores from Davis Pond in western Massachusetts also contain alternating layers of sand and organic-rich (high-LOI) silt above the 5.6 ka horizon (Figure 2e) [*Newby et al.*, 2011]. By applying our decision-tree approach, we find that the lake has experienced a long-term rise since >9.0 ka, which was punctuated by four major periods of drought since 5.6 ka (Figure 4). The relative magnitudes of the trend (+1 standard deviation of the >12.0 ka record since 6.0 ka) and multicentury low stands (−0.5 standard deviations) are comparable to those at NLP and Deep Pond, although not all of the changes are synchronous (Figure 4).

Based on LOI and X-radiography data [*Newby et al.*, 2011], sand layers or clusters of several layers extended to the deepest sediment core at Davis Pond during low water after 5.275, 4.375, 2.875, and 1.375 ka (Figure 4). Related sand deposition in nearshore cores (e.g., Figure 2E) began after 5.625 (5.725–5.275) ka.

3.4. Ages of Holocene Low-Lake Stands

Based on the ages of the sand layers at NLP, Deep Pond, and Davis Pond, the first multicentury episode of low water in western Massachusetts (Davis) was earlier than that recorded at the eastern lakes. The age distribution for the end of the first low stand at Davis Pond at 4.975 (5.025–4.625) ka overlaps with the beginning of the first low stand at NLP and Deep Pond at 4.925 (5.125–4.475) ka. The water level changes may have been out of phase between coastal and inland areas at 5.6–4.9 ka (Figure 4) like forest composition and potential temperature changes [*Foster et al*., 2006; *Marsicek et al*., 2013].

By contrast, the beginning of the four major low-water episodes at NLP and Deep Pond appears synchronous within our age uncertainties (Figure 3). The median ages for the low stands at each site fall within the 95% range of the ages from the other site. Furthermore, when we examine both the beginning and end of the low stands, we find that the low-water events at the two lakes overlap in time. Taken together, the timing of the events (i.e., the modal ages of onset and termination) at the two coastal lakes is 4.925–4.575, 4.225–3.875, 2.925–2.125, and 1.275–1.175 ka, which indicates durations of 350, 350, 800, and 100 years, respectively (Figure 4).

After 4.9 ka, the coastal and inland changes appear in phase with overlapping periods of low water (Figure 4). No significant differences exist for the ages of the three most recent low-water periods, which have modal ages of 4.375–4.125, 2.875–1.975, and 1.375–1.325 ka at Davis. Although the time between the modes of the beginning and end of the most recent low stand at Davis does not overlap with that from the eastern sites, the timing may have been synchronous (Figure 4) as the 95% age distribution for the onset of low water from Davis Pond core 100 (1.525–0.425 ka) overlaps with the ages from Deep Pond cores 16 and 10 (1.590–0.930 ka).

4. Discussion

4.1. Timing, Spatial Patterning, and Magnitude of Past Droughts

The similarities of the radar and physical sediment stratigraphies at multiple lakes in Massachusetts indicate that closely situated lakes, such as NLP and Deep Pond, experienced a related series of hydrologic changes (Figures 2 and 3). The quantified lake level reconstructions confirm that the lakes share 70% of the paleohydrologic variation on centennial-to-millennial timescales (Figure 3), and the statistical similarities of the ages of the lake level changes support this conclusion (Figures 3 and 4). The correlations and age agreements are high despite different hydrologic settings and differences associated with age uncertainties and limitations in reconstruction skill related to core spacing and sensitivity. For this reason, we infer that most of the shared variance is driven by regional climatic changes, such as an orbitally forced increase in effective moisture since >9.0 ka [*Shuman and Plank*, 2011] and centennial-scale droughts at ~4.9–4.6, 4.2–3.9, 2.9–2.1, and 1.3–1.1 ka (Figure 4).

Our data show that some of these changes extended across Massachusetts but that at least one event at ~5.6–4.9 ka exhibited a coastal-inland contrast over 200 km (Figure 4). Pollen data indicate that the thermal contrast between coastal and inland sites reached its Holocene maximum at this time and then was dramatically reduced at ~5.0 ka [*Marsicek et al*., 2013]. A rapid change in atmospheric circulation over the region at this time, such as inferred from oxygen isotope data [*Kirby et al*., 2002], may have favored the delivery and production of precipitation at the coast, possibly through onshore-offshore shifts in the tracking of Atlantic cyclones [*Bradbury et al*., 2003].

4.2. Comparison With North Atlantic Variability

Atmospheric circulation changes across the North Atlantic region, associated with the NAO on annual timescales, can influence effective moisture in eastern North America [*Seager et al*., 2012]. Similarly, we find that the timing of drought in Massachusetts coincided with cool episodes in Greenland [*Alley*, 2000] (Figure 4), which is consistent with large-scale pan-Atlantic dynamics. However, the correspondence of a cold Greenland and dry northeast U.S. during the past six millennia differs from the relationships associated with the NAO today [*Thompson and Wallace*, 2001; *Bradbury et al*., 2002; *Seager et al*., 2012]. Likewise, the timing of dry episodes observed here differ from the timing of geochemical events in Greenland ice cores that have been used as an index of NAO-like circulation changes during the Holocene [*O'Brien et al*., 1995].

Our data sets may capture regional expressions of a series of events that have often been discussed in isolation as prominent features of the Holocene climate record: climatic anomalies at ~4.2, 2.7, and 1.2 ka [*van Geel et al*., 2000; *Booth et al*., 2005; *Renssen et al*., 2006; *Martin-Puertas et al*., 2012]. Based on the core and

GPR data, these events represent enhanced hydrologic variability in the northeast U.S. after ~5.6 ka. Paleoceanographic data sets indicate similar centennial-to-millennial variability, including reductions in North Atlantic deepwater formation [*Oppo et al*., 2003] coincident with shifts in thermocline salinities and sea surface temperatures off Iceland [*Thornalley et al*., 2009] and West Africa [*deMenocal et al*., 2000]. Lake levels (and effective moisture) in Massachusetts were more likely to be lower than expected based on orbitally driven insolation trends during periods of reduced gyre circulation (e.g., a weak Canary Current; high gyre salinities) [*deMenocal et al*., 2000; *Thornalley et al*., 2009].

5. Conclusion

The similarity among lake stratigraphies emphasizes robust, climate-driven hydrologic variability on multicentury timescales, even where the lakes have differences in substrate, morphology, and hydrology, and where individual cores have differences in bathymetric location, sediment accumulation histories, and radiocarbon age control. The correlations among lake level reconstructions at closely situated lakes confirm both the presence of important hydrologic variability and the ability to use approaches such as those applied here to accurately reconstruct centennial and longer paleohydrologic changes.

The results are consistent with a sensitivity of the coastal northeast U.S. to the atmospheric or oceanic conditions in the North Atlantic region, but the dynamics involved in forcing these changes remains enigmatic. Such dynamics may include the amplification of weak external (e.g., solar) forcing, but this need not be so [*Renssen et al*., 2006; *Thornalley et al*., 2009; *van Geel et al*., 2000] and could indicate internal atmospheric variability integrated over centuries even if the dynamics involved exist on finer timescale [*Seager et al*., 2012]. In either case, our records confirm nonstationarity in regional conditions [*Milly et al*., 2008] and that water resources in the northeast U.S. have a low probability of remaining at current levels in coming decades and centuries.

Acknowledgments

The data for this paper are available at NOAA National Climate Data Center, http://ncdc.noaagov/data-access/paleo-climatology-data. The National Science Foundation (EAR-0602408, EAR-1036191, and DEB-0816731 to Shuman; EAR-0602380 to Donnelly) and the Woods Hole Oceanographic Institution, Ocean and Climate Change Institute (Donnelly) funded this research. Lake level reconstructions are programmed in R language and environment for statistical computing, Vienna, Austria. We thank K. Boldt, Z. Fjeldheim, M. Gomes, Z. Klaus, D. MacDonald, T. Miller, P. Pribyl, and R. Sorell for excellent field and laboratory work, L. Carlson at Brown University for GIS work, and two anonymous reviewers.

The Editor thanks two anonymous reviewers for their assistance in evaluating this paper.

References

Alley, R. B. (2000), The Younger Dryas cold interval as viewed from central Greenland, *Quat. Sci. Rev.*, *19*(1–5), 213–226.

Booth, R. K., S. T. Jackson, S. L. Forman, J. E. Kutzbach, E. A. Bettis, J. Kreig, and D. K. Wright (2005), A severe centennial-scale drought in midcontinental North America 4200 years ago and apparent global linkages, *Holocene*, *15*, 321.

Bradbury, J. A., S. L. Dingman, and B. D. Keim (2002), New England drought and relations with large scale atmospheric circulation patterns 1, *JAWRA J. Am. Water Resour. Assoc.*, *38*(5), 1287–1299, doi:10.1111/j.1752-1688.2002.tb04348.x.

Bradbury, J. A., B. D. Keim, and C. P. Wake (2003), The influence of regional storm tracking and teleconnections on winter precipitation in the Northeastern United States, *Ann. Assoc. Am. Geogr.*, *93*(3), 544–556, doi:10.1111/1467-8306.9303002.

Cook, E. R., R. Seager, M. A. Cane, and D. W. Stahle (2007), North American drought: Reconstructions, causes, and consequences, *Earth Sci. Rev.*, *81*(1–2), 93–134.

deMenocal, P., J. Ortiz, T. Guilderson, and M. Sarnthein (2000), Coherent high- and low-latitude climate variability during the Holocene warm period, *Science*, *288*(5474), 2198–2202, doi:10.1126/science.288.5474.2198.

Digerfeldt, G. (1986), Studies on past lake-level fluctuations, in *Handbook of Holocene Palaeoecology and Palaeohydrology*, edited by B. E. Berglund, pp. 127–142, John Wiley, Chichester, U. K.

Enfield, D. B., A. M. Mestas-Nuñez, and P. J. Trimble (2001), The Atlantic Multidecadal Oscillation and its relation to rainfall and river flows in the continental U.S., *Geophys Res Lett*, *28*(10), 2077–2080, doi:10.1029/2000gl012745.

Fawcett, P. J., et al. (2011), Extended megadroughts in the southwestern United States during Pleistocene interglacials, *Nature*, *470*(7335), 518–521.

Feng, S., Q. Hu, and R. Oglesby (2010), Influence of Atlantic sea surface temperatures on persistent drought in North America, *Clim. Dyn.*, *1–18*, doi:10.1007/s00382-010-0835-x.

Foster, D. R., W. W. Oswald, E. K. Faison, E. D. Doughty, and B. C. S. Hansen (2006), A climatic driver for abrupt mid-Holocene vegetation dynamics and the hemlock decline in New England, *Ecology*, *87*(12), 2959–2966.

Fritz, S. C., S. E. Metcalfe, and W. Dean (2000a), Holocene climate patterns in the Americas from paleolimnological records, in *Interhemispheric Climate Linkages*, edited by V. Markgraf, pp. 241–263, Academic Press, New York.

Fritz, S. C., E. Ito, Z. Yu, K. R. Laird, and D. Engstrom (2000b), Hydrologic variation in the northern Great Plains during the last two millennia, *Quat. Res.*, *53*, 175–184.

Harrison, S. P., and G. Digerfeldt (1993), European lakes as palaeohydrological and palaeoclimatic indicators, *Quat. Sci. Rev.*, *12*, 233–248.

Kirby, M. E., H. T. Mullins, W. P. Patterson, and A. W. Burnett (2002), Late glacial-Holocene atmospheric circulation and precipitation in the northeast United States inferred from modern calibrated stable oxygen and carbon isotopes, *Geol. Soc. Am. Bull.*, *114*(10), 1326–1340, doi:10.1130/0016-7606(2002)114<1326:LGHACA>2.0.CO;2.

Li, Y.-X., Z. Yu, and K. P. Kodama (2007), Sensitive moisture response to Holocene millennial-scale climate variations in the Mid-Atlantic region, USA, *Holocene*, *17*(1), 3–8, doi:10.1177/0959683606069386.

Marsicek, J. P., B. Shuman, S. Brewer, D. R. Foster, and W. W. Oswald (2013), Moisture and temperature changes associated with the mid-Holocene Tsuga decline in the northeastern United States, *Quat. Sci. Rev.*, *80*, 129–142, doi:10.1016/j.quascirev.2013.09.001.

Martin-Puertas, C., K. Matthes, A. Brauer, R. Muscheler, F. Hansen, C. Petrick, A. Aldahan, G. Possnert, and B. van Geel (2012), Regional atmospheric circulation shifts induced by a grand solar minimum, *Nat. Geosci.*, *5*(6), 397–401, doi:10.1038/ngeo1460.

Milly, P. C. D., J. Betancourt, M. Falkenmark, R. M. Hirsch, Z. W. Kundzewicz, D. P. Lettenmaier, and R. J. Stouffer (2008), Climate change: Stationarity is dead—Whither water management?, *Science*, *319*(5863), 573–574, doi:10.1126/science.1151915.

Mitchell, T. D., and P. D. Jones (2005), An improved method of constructing a database of monthly climate observations and associated high-resolution grids, *Int. J. Climatol.*, *25*(6), 693–712, doi:10.1002/joc.1181.
Namias, J. (1966), Nature and possible causes of the northeastern United States drought during 1962–65, *Mon. Weather Rev.*, *94*(9), 543–554.
Newby, P., J. P. Donnelly, B. N. Shuman, and D. MacDonald (2009), Evidence of centennial-scale drought from southeastern Massachusetts during the Pleistocene/Holocene transition, *Quat. Sci. Rev.*, *28*(17–18), 1675–1692.
Newby, P., B. N. Shuman, J. P. Donnelly, and D. MacDonald (2011), Repeated century-scale droughts over the past 13,000 years near the Hudson River watershed, U.S.A., *Quat. Res.*, *75*(3), 523–530.
O'Brien, S. R., P. Mayewski, L. D. Meeker, M. S. Twickler, and S. I. Whitlow (1995), Complexity of Holocene climate as reconstructed from a Greenland ice core, *Science*, *270*, 1962–1964.
Oppo, D. W., J. F. McManus, and J. L. Cullen (2003), Palaeo-oceanography: Deepwater variability in the Holocene epoch, *Nature*, *422*(6929), 277–277.
Parnell, A. C., J. Haslett, J. R. M. Allen, C. E. Buck, and B. Huntley (2008), A flexible approach to assessing synchroneity of past events using Bayesian reconstructions of sedimentation history, *Quat. Sci. Rev.*, *27*(1920), 1872–1885, doi:10.1016/j.quascirev.2008.07.009.
Pederson, N., A. R. Bell, E. R. Cook, U. Lall, N. Devineni, R. Seager, K. Eggleston, and K. P. Vranes (2013), Is an epic pluvial masking the water insecurity of the Greater New York City Region?, *J. Clim.*, *26*(4), 1339–1354, doi:10.1175/JCLI-D-11-00723.1.
Pribyl, P., and B. Shuman (2014), A computational approach to quaternary lake-level reconstruction applied in the Central Rocky Mountains, Wyoming, USA, *Quat. Res.*, doi:10.1016/j.yqres.2014.01.012.
Rayner, N. A., D. E. Parker, E. B. Horton, C. K. Folland, L. V. Alexander, D. P. Rowell, E. C. Kent, and A. Kaplan (2003), Global analyses of sea surface temperature, sea ice, and night marine air temperature since the late nineteenth century, *J. Geophys. Res.*, *108*(D14), 4407, doi:10.1029/2002JD002670.
Renssen, H., H. Goosse, and R. Muscheler (2006), Coupled climate model simulation of Holocene cooling events: Oceanic feedback amplifies solar forcing, *Clim. Past*, *2*, 79–90.
Seager, R., N. Pederson, Y. Kushnir, J. Nakamura, and S. Jurburg (2012), The 1960s drought and the subsequent shift to a wetter climate in the Catskill Mountains Region of the New York City Watershed, *J. Clim.*, *25*(19), 6721–6742, doi:10.1175/JCLI-D-11-00518.1.
Shuman, B. (2012), Patterns, processes, and impacts of abrupt climate change in a warm world: The past 11,700 years, *WIREs Clim Change*, *3*(1), 19–43, doi:10.1002/wcc.152.
Shuman, B., and J. P. Donnelly (2006), The influence of seasonal precipitation and temperature regimes on lake levels in Northeastern United States during the Holocene, *Quat. Res.*, *65*, 44–56.
Shuman, B., and B. Finney (2006), Late-Quaternary lake-level changes in North America, in *Encyclopedia of Quaternary Sciences*, edited by S. Elias, pp. 1374–1383, Elsevier, Amsterdam, Netherlands.
Shuman, B., and C. Plank (2011), Orbital, ice sheet, and possible solar controls on Holocene moisture trends in the North Atlantic drainage basin, *Geology*, *39*(2), 151–154, doi:10.1130/g31387.1.
Thompson, D. W. J., and J. M. Wallace (2001), Regional climate impacts of the Northern Hemisphere annular mode, *Science*, *293*(5527), 85–89, doi:10.1126/science.1058958.
Thornalley, D. J. R., H. Elderfield, and I. N. McCave (2009), Holocene oscillations in temperature and salinity of the surface subpolar North Atlantic, *Nature*, *457*(7230), 711–714.
Van Geel, B., C. J. Heusser, H. Renssen, and C. J. E. Schuurmans (2000), Climatic change in Chile at around 2700 BP and global evidence for solar forcing: A hypothesis, *Holocene*, *10*(5), 659–664, doi:10.1191/09596830094908.
Wanner, H., O. Solomina, M. Grosjean, S. P. Ritz, and M. Jetel (2011), Structure and origin of Holocene cold events, *Quat. Sci. Rev.*, *30*(21–22), 3109–3123, doi:10.1016/j.quascirev.2011.07.010.
Webb, R. S., K. H. Anderson, and T. Webb (1993), Pollen response-surface estimates of Late-Quaternary changes in the moisture balance of the Northeastern United States, *Quat. Res.*, *40*(2), 213–227.
Winter, T. C. (1999), Relation of streams, lakes, and wetlands to groundwater flow systems, *Hydrogeol. J.*, *7*(1), 28–45, doi:10.1007/s100400050178.